

## Anomalous dynamical scaling and bifractality in the one-dimensional Anderson model

This article has been downloaded from IOPscience. Please scroll down to see the full text article.

1998 J. Phys. A: Math. Gen. 31 7699

(<http://iopscience.iop.org/0305-4470/31/38/007>)

View [the table of contents for this issue](#), or go to the [journal homepage](#) for more

Download details:

IP Address: 171.66.16.102

The article was downloaded on 02/06/2010 at 07:12

Please note that [terms and conditions apply](#).

# Anomalous dynamical scaling and bifractality in the one-dimensional Anderson model

S De Toro Arias<sup>†§</sup> and J M Luck<sup>‡||</sup>

<sup>†</sup> Laboratoire de Physique de la Matière Condensée<sup>+</sup>, Université de Nice-Sophia-Antipolis, Parc Valrose, BP 71, 06108 Nice Cedex 2, France and CEA Saclay, Service de Physique de l'État Condensé, 91191 Gif-sur-Yvette Cedex, France

<sup>‡</sup> CEA Saclay, Service de Physique Théorique, 91191 Gif-sur-Yvette Cedex, France

Received 15 June 1998

**Abstract.** We investigate dynamical scaling properties of the one-dimensional tight-binding Anderson model with weak diagonal disorder, by means of the spreading of a wavepacket. In the absence of disorder, and more generally in the ballistic regime ( $t \ll \xi_0$  in reduced units, with  $\xi_0$  being the localization length near the band centre), the wavefunction exhibits sharp fronts. These ballistic fronts yield an anomalous time dependence of the  $q$ th moment of the local probability density, or dynamical participation number of order  $q$ , with a non-trivial exponent  $\tau(q)$  for  $q > 2$ . This striking feature is interpreted as bifractality. A heuristic treatment of the localized regime ( $t \gg \xi_0$ ) demonstrates a similar anomalous scaling, but with  $\xi_0$  replacing time. The moments of the position of the particle are not affected by the fronts, and obey normal scaling. The crossover behaviour of all these quantities between the ballistic and the localized regime is described by scaling functions of one single variable  $x = t/\xi_0$ . These predictions are confirmed by accurate numerical data, both in the normal and in the anomalous case.

## 1. Introduction

The Anderson localization in a random potential is now well understood, at least as far as static or spectral properties are concerned [1]. In the one-dimensional case, all eigenstates are exponentially localized, with the localization length  $\xi(E)$  depending on energy  $E$  [2, 3]. Dynamical aspects, concerning mostly the spreading of a wavepacket, have also recently attracted considerable interest [4–6], especially in connection with diffusion in driven quantum systems and random band matrices [7–9], and more recently with the problem of two interacting particles [10].

In this paper, we emphasize a novel and striking feature of the dynamics of the one-dimensional tight-binding Anderson model. The  $q$ th moment of the local probability density, or dynamical participation number of order  $q$ , to be defined in equation (1.4), exhibits anomalous scaling and bifractal behaviour, with a non-trivial exponent  $\tau(q)$  for  $q > 2$ . This phenomenon seems to have been entirely overlooked so far. It will be shown to take place in the absence of disorder, and in the ballistic regime, in the localized regime, and throughout the crossover between them.

<sup>§</sup> E-mail address: sdetoro@ondine.unice.fr

<sup>||</sup> Author to whom correspondence should be addressed. E-mail address: luck@spt.saclay.cea.fr

<sup>+</sup> UMR 6622 of CNRS.

To be more specific, we investigate the time-dependent wavefunction of a tight-binding electron in one dimension, which obeys

$$i \frac{d\psi_n(t)}{dt} = \psi_{n+1}(t) + \psi_{n-1}(t) + v_n \psi_n(t) \quad (1.1)$$

in reduced units, such that lengths are measured in units of the lattice spacing, and energies and inverse times in units of the hopping integral. The diagonal site potentials  $\{v_n\}$  are independent random variables, drawn from a common distribution. We choose the initial condition of a particle sitting at the site  $n = 0$  at the origin of times:

$$\psi_n(0) = \delta_{n,0}. \quad (1.2)$$

We characterize the spreading of the wavepacket by the following quantities.

- Moments of the position of the particle:

$$M_q(t) = \overline{|n|^q} = \sum_n |n|^q \overline{P_n(t)}. \quad (1.3)$$

- Moments of the probability density (dynamical participation numbers):

$$S_q(t) = \sum_n \overline{(P_n(t))^q}. \quad (1.4)$$

In the above definitions, the probability density reads

$$P_n(t) = |\psi_n(t)|^2 \quad (1.5)$$

and the index  $q$  is any real positive number, not necessarily an integer. The bar denotes an average over the disorder, i.e. over the distribution of the random site potentials  $\{v_n\}$ . The conservation of the norm of the wavefunction ensures that  $M_0(t) = S_1(t) = 1$  at all times  $t \geq 0$ . The most commonly considered quantities in the literature are the mean-squared position  $M_2(t)$  and the participation number (or inverse participation ratio)  $S_2(t)$  [11–13].

Scaling properties are known to hold in the weak-disorder regime, namely for a small enough random potential. Assuming that the site potentials have zero average, it is sufficient to characterize their distribution by its variance:

$$\overline{v_n} = 0 \quad \overline{v_n^2} = \sigma^2 \ll 1. \quad (1.6)$$

To lowest order in perturbation theory, the localization length is maximal in the vicinity of the band centre, where it scales as [1–3]

$$\xi_0 \approx \frac{8}{\sigma^2}. \quad (1.7)$$

This is the characteristic length scale where the localization phenomenon takes place. The absence of an intermediate diffusive regime between the ballistic one ( $t \ll \xi_0$ ) and the localized one ( $t \gg \xi_0$ ) is a peculiarity of the one-dimensional situation, where there is no fundamental difference between the mean free path and the localization length [14–18]. A more detailed description of the localization length, including its anomalous scaling near band edges, will be recalled in section 3.1.

We shall be interested in the long-time behaviour of the moments  $M_q(t)$  and  $S_q(t)$  defined above, in the weak-disorder regime. Scaling properties can be expected in this situation, where both characteristic length scales  $t$  and  $\xi_0$  are simultaneously large. The set-up of this paper is as follows. Section 2 contains a detailed analytical investigation of the problem in the absence of disorder. The wavefunction is given by a Bessel function, which exhibits three different kinds of asymptotic behaviour in the  $(n, t)$  plane. As a consequence, the moments  $S_q(t)$  of the probability density exhibit anomalous growth with a scaling exponent  $\tau(q)$  for  $q > 2$ . This behaviour, interpreted as bifractality, is expected

to hold in the ballistic regime, namely for  $t \ll \xi_0$ , where disorder will have hardly any effect on the ballistic motion of the particle in the absence of disorder. In section 3 we show on a heuristic basis that the same kind of anomalous scaling, with the same exponent  $\tau(q)$ , also takes place in the localized regime ( $t \gg \xi_0$ ), but with the asymptotic width of the wavepacket, of order  $\xi_0$ , replacing time. Finally, we demonstrate that all the quantities under consideration exhibit scaling behaviour throughout the crossover between the free (ballistic) and the localized (insulating) regimes, involving universal scaling functions of the variable  $x = t/\xi_0$ . This prediction is confirmed by accurate numerical data. Section 4 contains a brief discussion.

## 2. Analytical results in the absence of disorder

### 2.1. Description of the wavefunction

In the absence of disorder, the dynamics of the Anderson model can be investigated analytically. Let us denote the various quantities with the superscript (0) in this limiting case. The stationary tight-binding equation reads

$$\psi_{n+1}^{(0)} + \psi_{n-1}^{(0)} = E\psi_n^{(0)}. \quad (2.1)$$

Its eigenfunctions are the plane waves  $\psi_n^{(0)} = e^{inp}$ , where momentum  $p$  is related to energy  $E$  by the dispersion relation

$$E = 2 \cos p. \quad (2.2)$$

We thus obtain an explicit expression for the time-dependent wavefunction,

$$\psi_n^{(0)}(t) = \int_B \frac{dp}{2\pi} e^{inp-2it \cos p} = i^{-n} J_n(2t) \quad (2.3)$$

where the momentum integral runs over the Brillouin zone  $B = [-\pi, \pi]$ . The probability density at site  $n$ ,

$$P_n^{(0)}(t) = |\psi_n^{(0)}(t)|^2 = (J_n(2t))^2 \quad (2.4)$$

is thus the square of the Bessel function  $J_n(2t)$ , whose argument is proportional to time, while its order is the number of the site, i.e. the distance travelled by the particle from its starting point.

It turns out that three regions have to be considered in the  $(n, t)$  plane, where the Bessel function admits different kinds of asymptotic behaviour. The existence of these regions can be explained by the following semi-classical argument. The dispersion relation (2.2) corresponds to the group velocity  $v = dE/dp = -2 \sin p$ . As a consequence, for a wavepacket initially peaked in momentum space around some mean  $p_*$ , the centre of mass will move according to the semi-classical law

$$\langle n \rangle \approx -2t \sin p_*. \quad (2.5)$$

We thus expect an allowed region ( $|n| < 2t$ ), separated from a forbidden region ( $|n| > 2t$ ) by sharp fronts located at  $n \approx \pm 2t$ .

The above heuristic picture can be made quantitative by means of the following asymptotic formulae in the theory of Bessel functions [19]. As a matter of fact, the derivation of these formulae relies on the method of steepest descent, with the saddle-point equation coinciding with equation (2.5).

- Allowed region ( $|n| < 2t$ ).

For  $n > 0$ , and with the notation

$$n = 2t \sin p \quad (0 < p < \pi/2) \quad (2.6)$$

in agreement with the semi-classical law (2.5), we have

$$P_n^{(0)}(t) \approx \frac{\sin^2(n(p + \cot p - \pi/2) + \pi/4)}{\pi t \cos p}. \quad (2.7)$$

The probability density is thus the product of  $1/t$  by a rapidly oscillating amplitude, as expected in an allowed region.

- Forbidden region ( $|n| > 2t$ ).

For  $n > 0$ , and with the notation

$$n = 2t \cosh \theta \quad (\theta > 0) \quad (2.8)$$

we have

$$P_n^{(0)}(t) \approx \frac{\exp(-2n(\theta - \tanh \theta))}{4\pi t \sinh \theta}. \quad (2.9)$$

The probability density thus decays exponentially, as expected in a forbidden region.

- Transition region ( $|n| \approx 2t$ ).

The transition region, corresponding to the ballistic fronts, turns out to extend over a spatial range of order  $t^{1/3}$ . For  $n > 0$ , and with the notation

$$n = 2t + t^{1/3}z \quad (2.10)$$

the probability density is approximated as

$$P_n^{(0)}(t) \approx t^{-2/3} (\text{Ai}(z))^2 \quad (2.11)$$

with  $\text{Ai}(z)$  being the Airy function. The asymptotic behaviour of this function, namely

$$\text{Ai}(z) \approx \begin{cases} \pi^{-1/2} |z|^{-1/4} \sin(\frac{2}{3}|z|^{3/2} + \frac{\pi}{4}) & (z \rightarrow -\infty) \\ \frac{1}{2} \pi^{-1/2} z^{-1/4} \exp(-\frac{2}{3}z^{3/2}) & (z \rightarrow +\infty) \end{cases} \quad (2.12)$$

respectively matches equations (2.7) and (2.9).

Throughout the transition region, the probability density is the product of  $t^{-2/3}$  by an amplitude which oscillates toward the allowed region ( $z \rightarrow -\infty$ ), and falls off exponentially toward the forbidden region ( $z \rightarrow +\infty$ ).

The existence of these three regions is illustrated in figure 1, showing the probability density  $P_n^{(0)}(t)$  against site number  $n$ , for a time  $t = 100$ .

## 2.2. Moments of the position

We now turn to the analysis of the moments  $M_q^{(0)}(t)$  of the position of the particle, in the absence of disorder. These quantities are quadratic forms in Bessel functions, so that their analysis is rather easy, at least for even integer values of the index:  $q = 2k$ . We have indeed

$$\begin{aligned} M_{2k}^{(0)}(t) &= \sum_n n^{2k} (J_n(2t))^2 \\ &= \int_B \frac{dp}{2\pi} \int_B \frac{dp'}{2\pi} e^{2it(\cos p' - \cos p)} \underbrace{\sum_n n^{2k} e^{in(p-p')}}_{2\pi \left(-i \frac{d}{dp}\right)^{2k} \delta(p-p')} \\ &= \int_B \frac{dp}{2\pi} e^{-2it \cos p} \left(-\frac{d^2}{dp^2}\right)^k e^{2it \cos p}. \end{aligned} \quad (2.13)$$

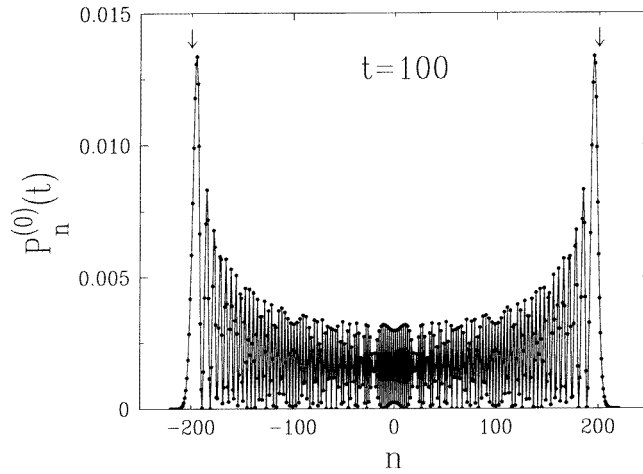


**Figure 1.** Plot of the probability density  $P_n^{(0)}(t) = (J_n(2t))^2$  in the absence of disorder, against site number  $n$ , for a time  $t = 100$ . Arrows indicate the semi-classical ballistic fronts at  $n = \pm 200$ .

The integrand of the last expression can be expanded as a trigonometric polynomial. As a result, the moments  $M_{2k}^{(0)}(t)$  are even polynomials of  $t$ , with positive integer coefficients. We have  $M_0^{(0)}(t) = 1$ , as expected, and

$$M_2^{(0)}(t) = 2t^2 \quad M_4^{(0)}(t) = 6t^4 + 2t^2 \quad M_6^{(0)}(t) = 20t^6 + 30t^4 + 2t^2 \quad \text{etc.} \quad (2.14)$$

The long-time behaviour of the moments is obtained by letting all the derivatives act on the exponential in the last expression of equation (2.13). We thus obtain

$$M_{2k}^{(0)}(t) \approx a_{2k} t^{2k} \quad (t \gg 1) \quad (2.15)$$

with

$$a_{2k} = \int_B \frac{dp}{2\pi} (4 \sin^2 p)^k = \frac{(2k)!}{(k!)^2}. \quad (2.16)$$

This estimate can be shown to hold true for any real  $q > 0$ , namely

$$M_q^{(0)}(t) \approx a_q t^q \quad (t \gg 1) \quad (2.17)$$

with

$$a_q = \frac{2^q}{\pi^{1/2}} \frac{\Gamma\left(\frac{q+1}{2}\right)}{\Gamma\left(\frac{q+2}{2}\right)} \quad (2.18)$$

where  $\Gamma(z)$  denotes Euler's gamma function.

### 2.3. Moments of the probability density (participation numbers)

The analysis of the long-time behaviour of the moments  $S_q^{(0)}(t)$  of the probability density is slightly more involved. Indeed these quantities are highly nonlinear functionals of the wavefunction. As the index  $q$  gets larger, they are more and more sensitive to large values of the wavefunction, whereas the moments  $M_q^{(0)}(t)$  of the position are not.

The asymptotic expressions (2.7), (2.9), (2.11) show that the probability density  $P_n^{(0)}(t)$  scales as  $1/t$  in the allowed region (bulk of the wavefunction), over an extent of order  $t$  sites,

**Table 1.** Summary of various characteristic features of the bifractality phenomenon.

Component of bifractality	Normal	Anomalous
Relevant region of wavefunction in ballistic regime ( $t \ll \xi_0$ )	Bulk (allowed region) $P_n(t) \sim t^{-1}$	Fronts (transition region) $P_n(t) \sim t^{-2/3}$
Relevant eigenstates in localized regime ( $t \gg \xi_0$ )	Bulk of spectrum $\xi \sim \xi_0 \sim \sigma^{-2}$	Band edges $\xi \sim \sigma^{-2/3}$
Range of index $q$	$q < 2$	$q > 2$
Exponent $\tau(q)$	$q - 1$	$\frac{2q-1}{3}$
Rényi dimension $D_q$	1	$\frac{2q-1}{3(q-1)}$
Multifractal spectrum	$\alpha = 1, f = 1$	$\alpha = \frac{2}{3}, f = \frac{1}{3}$

while it scales as  $t^{-2/3}$  in the transition region (fronts of the wavefunction), over an extent of order  $t^{1/3}$  sites, and it is negligible in the forbidden region (tails of the wavefunction). Hence the bulk has a normal contribution to the moment  $S_q^{(0)}(t)$ , scaling as  $t^{-(q-1)}$ , while the anomalous contribution of the fronts scales as  $t^{-(2q-1)/3}$ . This analysis therefore predicts the power-law behaviour

$$S_q^{(0)}(t) \approx b_q t^{-\tau(q)} \quad (t \gg 1) \quad (2.19)$$

with  $\tau(q)$  being the smaller of both exponents, namely

$$\tau(q) = \begin{cases} q - 1 & \text{for } q < 2 \text{ (normal)} \\ \frac{2q - 1}{3} & \text{for } q > 2 \text{ (anomalous)}. \end{cases} \quad (2.20)$$

This prediction is summarized in table 1. It can be made more quantitative by the following analysis, yielding the value of the prefactor  $b_q$  of the formula (2.19) in either case.

- Normal regime ( $q < 2$ ).

In the normal regime, the moment  $S_q^{(0)}(t)$  is dominated by the bulk of the wavefunction, corresponding to the allowed region. The prefactor of equation (2.19) can be estimated from the expression (2.7), assuming that the arguments of the sine functions are uniformly distributed, and transforming the sum over  $n$  into an integral over  $p$ . We thus obtain after some algebra  $S_q^{(0)}(t) \approx b_q t^{-(q-1)}$ , in agreement with equation (2.20), with

$$b_q = \frac{2}{\pi^q} \frac{\Gamma\left(\frac{2-q}{2}\right) \Gamma\left(q + \frac{1}{2}\right)}{\Gamma\left(\frac{3-q}{2}\right) \Gamma(q+1)} \quad (q < 2). \quad (2.21)$$

- Anomalous regime ( $q > 2$ ).

In the anomalous regime, the moment  $S_q^{(0)}(t)$  is dominated by the fronts of the wavefunction, corresponding to the transition region. The prefactor of this moment can then be estimated by using the expression (2.11), and transforming the sum over  $n$  into an integral over  $z$ . The outcome again agrees with equation (2.20), and yields

$$b_q = 2 \int_{-\infty}^{+\infty} dz |\text{Ai}(z)|^{2q} \quad (q > 2). \quad (2.22)$$

We have in particular

$$b_3 = 0.073\,214. \quad (2.23)$$

- Marginal case ( $q = 2$ ).

This borderline case corresponds to the usual participation number  $S_2(t)$ . The exponents of the contributions of the bulk and of the fronts have the common value  $\tau(2) = 1$ . It is worth noting that the prefactor  $b_q$  diverges as  $b_q \approx 3/(2\pi^2|q - 2|)$  as  $q \rightarrow 2$  from both sides. This can be checked for  $q < 2$  directly from equation (2.21), and for  $q > 2$  from the behaviour (2.12) of the Airy function as  $z \rightarrow -\infty$ .

The moment  $S_2^{(0)}(t)$  turns out to exhibit a logarithmic correction to its leading  $1/t$  behaviour, which can be analysed by means of the Mellin transformation. The function  $S_2^{(0)}(t)$  and its Mellin transform  $m(s)$  are related by

$$m(s) = \int_0^\infty t^{s-1} S_2^{(0)}(t) dt \quad S_2^{(0)}(t) = \int \frac{ds}{2\pi i} t^{-s} m(s) \tag{2.24}$$

for  $\text{Re } s$  positive and small enough. We have

$$\begin{aligned} S_2^{(0)}(t) &= \sum_n (J_n(2t))^4 \\ &= \int_B \frac{dp_1}{2\pi} \dots \int_B \frac{dp_4}{2\pi} e^{2it(\cos p_1 + \cos p_2 - \cos p_3 - \cos p_4)} \underbrace{\sum_n e^{in(p_3 + p_4 - p_1 - p_2)}}_{2\pi \delta(p_1 + p_2 - p_3 - p_4)} \\ &= \int_B \frac{du}{2\pi} \int_B \frac{dv}{2\pi} \int_B \frac{dw}{2\pi} e^{-8it \sin u \sin v \sin w} \end{aligned} \tag{2.25}$$

where the last expression has been obtained by the change of variables

$$\begin{aligned} u &= (p_1 - p_2 + p_3 - p_4)/4 & v &= (p_1 - p_2 - p_3 + p_4)/4 \\ w &= (\pi - p_1 - p_2)/2 = (\pi - p_3 - p_4)/2. \end{aligned} \tag{2.26}$$

The product structure of the last expression of equation (2.25) makes it suitable to the closed-form evaluation of the Mellin transform  $m(s)$ . We indeed obtain, for  $0 < \text{Re } s < 1$ ,

$$\begin{aligned} m(s) &= \Gamma(s) \int_B \frac{du}{2\pi} \int_B \frac{dv}{2\pi} \int_B \frac{dw}{2\pi} (8i \sin u \sin v \sin w)^{-s} \\ &= \Gamma(s) 8^{-s} \cos \frac{s\pi}{2} \left( \int_B \frac{du}{2\pi} |\sin u|^{-s} \right)^3 \\ &= \Gamma(s) 8^{-s} \cos \frac{s\pi}{2} \left( \frac{\Gamma(\frac{1-s}{2})}{\pi^{1/2} \Gamma(\frac{2-s}{2})} \right)^3. \end{aligned} \tag{2.27}$$

The long-time behaviour of  $S_2^{(0)}(t)$  is given by the double-pole singularity of  $m(s)$  at  $s = 1$ , of the form

$$m(s) = \frac{1}{2\pi^2} \left( \frac{1}{(1-s)^2} + \frac{6 \ln 2 + \gamma_E}{1-s} + \dots \right) \tag{2.28}$$

where  $\gamma_E$  denotes Euler's constant, hence

$$S_2^{(0)}(t) \approx \frac{\ln t + 6 \ln 2 + \gamma_E}{2\pi^2 t} \quad (t \gg 1). \tag{2.29}$$

We have thus derived both the prefactor and the finite part of the logarithmic correction of the dynamical participation number  $S_2^{(0)}(t)$  in the absence of disorder. The finite part is a surprisingly large number: writing the numerator of equation (2.29) as  $\ln(t/t_0)$ , we have  $1/t_0 = 64 \exp(\gamma_E) = 113.989$ .



#### 2.4. Interpretation: bifractality of the probability density

The scaling law (2.19), (2.20) for the moments  $S_q^{(0)}(t)$  of the probability density in the absence of disorder, with its two branches of exponent  $\tau(q)$ , can be interpreted within the multifractal formalism [20]. Indeed, the wavefunction takes appreciable values over a number of lattice sites of order  $t$ . As a consequence,  $1/t$  can be viewed as a short-distance cut-off in the definition (1.4) of the moments  $S_q(t)$ .

The scaling exponent  $\tau(q)$  can be interpreted in terms of generalized (Rényi) dimensions  $D_q$  of the local probability density. The relation  $\tau(q) = (q - 1)D_q$  yields

$$D_q = \begin{cases} 1 & \text{for } q < 2 \text{ (normal)} \\ \frac{2q - 1}{3(q - 1)} & \text{for } q > 2 \text{ (anomalous)}. \end{cases} \quad (2.30)$$

The probability density can be alternatively characterized by a multifractal spectrum  $f(\alpha)$ , which is the Legendre transform of the exponent  $\tau(q)$ , according to

$$\alpha = \frac{d\tau}{dq} \quad f = q \frac{d\tau}{dq} - \tau. \quad (2.31)$$

The expression (2.20) yields the following results. The normal branch  $\tau(q) = q - 1$ , i.e.  $D_q = 1$ , for  $q < 2$  yields the point  $(\alpha = 1, f = 1)$ , corresponding to the normal scaling of the bulk of the wavefunction, while the anomalous branch  $\tau(q) = (2q - 1)/3$  for  $q > 2$  yields the point  $(\alpha = \frac{2}{3}, f = \frac{1}{3})$ , corresponding to the anomalous scaling of the fronts of the wavefunction.

These results are summarized in table 1. We propose to call bifractality such a scaling behaviour, with a normal and an anomalous component.

### 3. Scaling analysis in the general case

#### 3.1. A reminder on band-edge anomalous scaling

We first recall some results on the scaling behaviour of the localization length in the presence of a weak diagonal disorder. Inside the band of the pure system, characterized by the dispersion relation (2.2), and in the weak-disorder regime ( $\sigma^2 \ll 1$ ), the localization length scales as [1–3]

$$\xi \approx \frac{8 \sin^2 p}{\sigma^2} \approx \xi_0 \sin^2 p. \quad (3.1)$$

This leading-order perturbative prediction vanishes as  $p \rightarrow 0$  or  $p \rightarrow \pi$ , corresponding to the band edges, namely  $E \rightarrow \pm 2$ . This observation suggests that the localization phenomenon has something special near band edges. This effect has been initially investigated by Derrida and Gardner [21], who indeed demonstrated the presence of anomalous scaling in the localization length  $\xi(E)$  and the density of states  $\rho(E)$ . These quantities behave near the upper band edge ( $E \rightarrow 2, \sigma \rightarrow 0$ ) as

$$\xi \approx \sigma^{-2/3} \Phi_1(\sigma^{-4/3}(E - 2)) \quad \rho \approx \sigma^{-2/3} \Phi_2(\sigma^{-4/3}(E - 2)) \quad (3.2)$$

where the scaling functions  $\Phi_1$  and  $\Phi_2$  are known analytically.

Roughly speaking, the eigenstates whose energy lies near the band edges have a localization length of order  $\sigma^{-2/3}$ . These states are therefore much more localized than typical eigenstates within the band, whose localization length is of order  $\xi_0 \sim \sigma^{-2}$ . Only a small fraction of the whole spectrum, of order  $\sigma^{2/3}$  or  $\xi_0^{-1/3}$ , consists of these anomalously localized eigenstates.

3.2. Heuristic analysis of the localized regime

We now turn to a heuristic investigation of the moments of the position and of the probability density, in the presence of a weak diagonal disorder, and in the localized regime ( $t \gg \xi_0 \gg 1$ ).

Consider for definiteness the Anderson model on a very long chain made of  $N \gg 1$  sites, for a given realization of the random potentials  $\{v_n\}$ . Let  $E^\alpha$  be the energy eigenvalues, labelled in some way by an integer  $\alpha$ , and  $\psi_n^\alpha$  be the corresponding eigenvectors. We have

$$\sum_n \psi_n^\alpha \psi_n^\beta = \delta^{\alpha,\beta} \quad \sum_\alpha \psi_m^\alpha \psi_n^\alpha = \delta_{m,n}. \quad (3.3)$$

We define the centre-of-mass coordinate  $n_{\text{cm}}^\alpha$  and the localization length  $\xi^\alpha$  of every eigenstate as

$$n_{\text{cm}}^\alpha = \sum_n n (\psi_n^\alpha)^2 \quad \xi^\alpha = \left( \sum_n (n - n_{\text{cm}}^\alpha)^2 (\psi_n^\alpha)^2 \right)^{1/2}. \quad (3.4)$$

The initial condition (1.2) can be expanded as  $\psi_n(0) = \delta_{n,0} = \sum_\alpha \psi_n^\alpha \psi_0^\alpha$ . As a consequence, the wavefunction reads at all times  $t \geq 0$

$$\psi_n(t) = \sum_\alpha e^{-iE^\alpha t} \psi_n^\alpha \psi_0^\alpha. \quad (3.5)$$

3.2.1. Moments of the position. Let us first take the example of the mean-squared position, for which equation (3.5) yields

$$M_2(t) = \sum_{\alpha,\beta} e^{-i(E^\alpha - E^\beta)t} \psi_0^\alpha \psi_0^\beta \sum_n n^2 \psi_n^\alpha \psi_n^\beta. \quad (3.6)$$

Our heuristic analysis of this expression will be based on the following two hypotheses.

(A) Interference terms between different quantum states can be neglected for large enough times. Equation (3.6) thus becomes in the localized regime

$$M_2(\infty) \approx \sum_\alpha (\psi_0^\alpha)^2 \sum_n n^2 (\psi_n^\alpha)^2. \quad (3.7)$$

(B) Scaling properties of eigenstates can be modelled by considering that the probability density  $(\psi_n^\alpha)^2$  is roughly uniform over the range  $|n - n_{\text{cm}}^\alpha| < \xi^\alpha$ . This simple scaling hypothesis has been shown by analytical means to hold in a variety of models, including random band matrices [7, 8], and the continuum Schrödinger equation in one dimension [13]. It amounts to stating that single eigenstates of the one-dimensional Anderson model do not exhibit multifractality, in contrast with earlier claims based on numerical evidence [22].

Consider first an eigenstate localized near the origin ( $|n_{\text{cm}}^\alpha| \ll \xi^\alpha$ ). For such an eigenstate, we have  $\sum_n n^2 (\psi_n^\alpha)^2 \sim (\xi^\alpha)^2$ , while the prefactor  $(\psi_0^\alpha)^2$  scales as  $1/\xi^\alpha$ . Now, in a small energy interval  $\Delta E$  around some energy  $E$ , there are altogether  $N\rho(E)\Delta E$  eigenstates, among which only a finite number, of order  $\xi(E)\rho(E)\Delta E$ , have  $|n_{\text{cm}}^\alpha| \sim \xi^\alpha$ . All these eigenstates bring comparable contributions, of order  $(\xi(E))^2$ , to the sum in equation (3.7). It is worth noting that the factor  $\xi(E)$  in the number of relevant eigenstates just compensates the prefactor  $(\psi_0^\alpha)^2 \sim 1/\xi^\alpha$ . We are thus left with the estimate

$$M_2(\infty) \sim \langle (\xi^\alpha)^2 \rangle_\alpha \quad (3.8)$$

where the angular brackets denote an average over the whole spectrum of eigenstates  $\alpha$ . More explicitly,

$$M_2(\infty) \sim \int (\xi(E))^2 \rho(E) dE \sim \xi_0^2. \quad (3.9)$$

We thus obtain the physically intuitive result that the mean-squared position saturates to a value of order  $\xi_0^2$  for  $t \gg \xi_0$ . Generalizing the above argument, we get the asymptotic result

$$M_q(\infty) \approx A_q \xi_0^q \quad (3.10)$$

for all the moments of the position, deep in the localized regime.

This prediction can actually be made quantitative, using results from the Russian literature [14–17]. The long-time density correlation function has been calculated in these references, for the continuum Schrödinger equation with a weak white-noise potential. If the initial wavepacket is peaked in energy around some mean  $E$ , one has  $M_q(\infty) \approx p_q (2\xi(E))^q$ , with the notation of [16], where the amplitudes  $p_q$  have been calculated analytically, for integer values of  $q$ . In the present situation, by averaging this prediction over the whole spectrum of energies, we recover equation (3.10), with

$$A_q = p_q \int_B \frac{dp}{2\pi} (2 \sin^2 p)^q. \quad (3.11)$$

We have in particular

$$A_2 = \frac{3\zeta(3)}{4} = 0.901543 \quad A_4 = \frac{7(180\zeta(5) + \pi^4)}{128} = 15.5343 \quad \text{etc} \quad (3.12)$$

where  $\zeta$  denotes Riemann's zeta function.

**3.2.2. Moments of the probability density (participation numbers).** Let us now turn to the more interesting case of the moments  $S_q(t)$  of the probability density, with  $q = 2, 3, \dots$  being an integer. Equation (3.5) and hypothesis (A) yield

$$S_q(\infty) \approx \sum_{\alpha_1, \dots, \alpha_q} (\psi_0^{\alpha_1})^2 \dots (\psi_0^{\alpha_q})^2 \sum_n (\psi_n^{\alpha_1})^2 \dots (\psi_n^{\alpha_q})^2. \quad (3.13)$$

Let us assume that the eigenstates  $\alpha_1, \dots, \alpha_q$  are ordered according to increasing localization lengths:  $\xi^{\alpha_1} < \xi^{\alpha_2} < \dots < \xi^{\alpha_q}$ , and employ again hypothesis (B). If all the  $q$  eigenstates have their centre-of-mass coordinates close enough to the origin ( $|n_{\text{cm}}^{\alpha_k}| \ll \xi^{\alpha_k}$  for  $k = 1, \dots, q$ ), the product  $(\psi_n^{\alpha_1})^2 \dots (\psi_n^{\alpha_q})^2$  is non-zero where the  $q$  eigenfunctions have a good common overlap. This occurs in the intersection of all their ranges, i.e. for  $|n| < \xi^{\alpha_1}$ , where the product is of order  $1/(\xi^{\alpha_1} \xi^{\alpha_2} \dots \xi^{\alpha_q})$ , while the sum over  $n$  brings a factor of  $\xi^{\alpha_1}$ . Here again, the number of relevant eigenstates in some energy range  $\Delta E$  cancels out with the prefactors  $(\psi_0^{\alpha_1})^2 \dots (\psi_0^{\alpha_q})^2$ , whence the estimate

$$S_q(\infty) \sim \left\langle \frac{1}{\xi^{\alpha_2} \dots \xi^{\alpha_q}} \right\rangle_{\alpha_1, \dots, \alpha_q}. \quad (3.14)$$

The averaging of this expression over the eigenstates  $\alpha_1, \dots, \alpha_q$  is more subtle than in the case of equation (3.8), since negative powers of the localization lengths are involved. Hence the anomalously localized eigenstates near the band edges can, and indeed will, play a role.

- If all the eigenstates  $\alpha_1, \dots, \alpha_q$  belong to the bulk of the spectrum, their localization lengths scale as  $\xi_0$ , and we obtain the normal prediction  $S_q(\infty) \sim \xi_0^{-(q-1)}$ .

- If, on the contrary, some of the eigenstates, namely  $\alpha_1, \dots, \alpha_m$ , with  $m \geq 1$ , belong to the band edges, while  $\alpha_{m+1}, \dots, \alpha_q$  belong to the bulk of the spectrum, the quantity to be averaged now scales as  $\xi_0^{-(m-1)/3-(q-m)}$ , while the total fraction of such  $q$ -uples of eigenstates is of order  $\xi_0^{-m/3}$ . The optimal choice of the number  $m$  of anomalous eigenstates is  $m = q$ , hence the anomalous estimate  $S_q(\infty) \sim \xi_0^{-(2q-1)/3}$ .

The exponents of the above two estimates coincide with those obtained in section 2.3 in the absence of disorder, with the localization length scale  $\xi_0$  replacing time, the bulk of the spectrum replacing the allowed region, and the band edges replacing the ballistic fronts. Generalizing the above reasoning to non-integer values of the index  $q$ , we predict the power-law behaviour

$$S_q(\infty) \approx B_q \xi_0^{-\tau(q)} \quad (\xi_0 \gg 1) \tag{3.15}$$

for the participation numbers in the localized regime, with the exponent  $\tau(q)$  being given in equation (2.20) and in table 1. Finally, in analogy with the result (2.29) in the absence of disorder, a logarithmic correction of the form

$$S_2(\infty) \approx \frac{\lambda \ln \xi_0 + \mu}{\xi_0} \quad (\xi_0 \gg 1) \tag{3.16}$$

is expected in the marginal case ( $q = 2$ ) of the usual participation number. The values of the prefactors  $B_q$ , and  $\lambda$  and  $\mu$  cannot be predicted by this heuristic analysis.

### 3.3. Scaling laws in the crossover regime

So far, we have obtained two kinds of predictions concerning the moments  $M_q(t)$  of the position of the particle and  $S_q(t)$  of the probability density in the weak-disorder regime. On the one hand, the analytical results (2.17), (2.19) obtained in the absence of disorder are expected to hold more generally in the ballistic regime, i.e. for  $1 \ll t \ll \xi_0$ . On the other hand, a heuristic scaling analysis led us to the predictions (3.10), (3.15) in the localized regime, i.e. for  $1 \ll \xi_0 \ll t$ .

It turns out that the exponents involved in these results always match between the ballistic and the localized regime, both in the normal and in the anomalous case. We are thus led to conjecture that the crossover between these two limiting situations is described by universal scaling functions of the single variable

$$x = \frac{t}{\xi_0} \tag{3.17}$$

throughout the scaling region where  $t$  and  $\xi_0$  are simultaneously large, with the ballistic regime corresponding to  $x \ll 1$ , and the localized regime to  $x \gg 1$ . It is worthwhile to recall that the absence of an intermediate diffusive regime between the ballistic one and the localized one is a peculiarity of the one-dimensional geometry.

*3.3.1. Moments of the position.* We thus propose the following one-variable scaling law for the moments of the position of the particle:

$$M_q(t) \approx a_q t^q F_q(x) \tag{3.18}$$

where the amplitudes  $a_q$  are as in equation (2.18). The result (2.17) in the absence of disorder is recovered as  $F_q(0) = 1$ , while the estimate (3.10) in the localized regime implies the power-law fall-off

$$F_q(x) \approx \frac{A_q}{a_q} x^{-q} \quad (x \gg 1). \tag{3.19}$$

The scaling law (3.18) can be shown to hold as  $x \ll 1$ , by means of a direct perturbative expansion in the random potentials [23]. This approach, following the lines of [24, 3], yields

$$F_q(x) = 1 - a_q^{(1)} x + \dots \quad (x \ll 1) \tag{3.20}$$

at least when the index  $q = 2k$  is an even integer, and in particular

$$a_2^{(1)} = \frac{32}{3\pi} = 3.395\,31 \quad a_4^{(1)} = \frac{1216}{135\pi} = 2.867\,15 \quad \text{etc.} \quad (3.21)$$

The analysis of the continuum Schrödinger equation [17] yields a behaviour similar to equation (3.20) at small  $x$ , as well as a singular correction of relative order  $(\ln x)/x$  to the leading power law (3.19) at large  $x$ . This logarithmic correction has been included in the analysis of numerical data on large random band matrices [9].

*3.3.2. Moments of the probability density (participation numbers).* Similarly, we postulate the following one-variable scaling laws for the moments of the probability density

$$S_q(t) \approx b_q t^{-\tau(q)} G_q(x) \quad (q \neq 2) \quad (3.22)$$

where the amplitudes  $b_q$  are as in equation (2.21) in the normal regime ( $q < 2$ ), and as in equation (2.22) in the anomalous regime ( $q > 2$ ). The result (2.19) is recovered as  $G_q(0) = 1$ , while the estimate (3.15) implies the power-law behaviour

$$G_q(x) \approx \frac{B_q}{b_q} x^{\tau(q)} \quad (x \gg 1). \quad (3.23)$$

In the marginal case of the usual participation number  $S_2(t)$ , we expect a logarithmic correction of the form

$$S_2(t) \approx \frac{\phi(x) \ln t + \chi(x)}{t}. \quad (3.24)$$

The result (2.29) in the absence of disorder is recovered as

$$\phi(0) = \frac{1}{2\pi^2} = 0.050\,660 \quad \chi(0) = \frac{6 \ln 2 + \gamma_E}{2\pi^2} = 0.239\,933 \quad (3.25)$$

while the estimate (3.16) in the localized regime implies

$$\phi(x) \approx \lambda x \quad \chi(x) \approx (\mu - \lambda \ln x)x \quad (x \gg 1). \quad (3.26)$$

### 3.4. Numerical results

In order to confirm the scaling predictions of section 3.3, we have performed direct numerical simulations of the dynamics of the tight-binding Anderson model. Introducing a finite timestep  $\varepsilon$ , we have discretized equation (1.1) into the difference equation

$$\psi_n(t + \varepsilon) = \psi_n(t - \varepsilon) - 2i\varepsilon(\psi_{n+1}(t) + \psi_{n-1}(t) + v_n \psi_n(t)). \quad (3.27)$$

In the absence of disorder, the dispersion relation of the corresponding stationary equation between energy  $E$  and momentum  $p$  now reads

$$\sin(\varepsilon E) = 2\varepsilon \cos p. \quad (3.28)$$

For a fixed momentum  $p$ , equation (3.28) has a first solution  $E^{(1)} = 2 \cos p + (4\varepsilon^2/3) \cos^3 p + \dots$  that smoothly converges toward the continuous-time expression (2.2), and a second solution  $E^{(2)} = \pi/\varepsilon - E^{(1)}$  modulo  $2\pi/\varepsilon$ , corresponding to fast oscillations over a timescale  $\varepsilon$ .

We have taken the initial condition (1.2) at time  $t = 0$ , while we have chosen at time  $t = \varepsilon$  the Taylor expansion of the solution of equation (1.1), to second order in  $\varepsilon$  included. The only non-zero components in the full initial condition read

$$\begin{aligned} \psi_0(0) &= 1 & \psi_0(\varepsilon) &= 1 - iv_0\varepsilon - (1 + v_0^2/2)\varepsilon^2 \\ \psi_{\pm 1}(\varepsilon) &= -i\varepsilon - (v_0 + v_{\pm 1})\varepsilon^2/2 & \psi_{\pm 2}(\varepsilon) &= -\varepsilon^2/2. \end{aligned} \quad (3.29)$$

This prescription reduces to the level of  $\varepsilon^3$  the amplitude of the fast oscillations related to the  $E^{(2)}$  branch of the dispersion relation (3.28).

We want to emphasize that the discrete-time difference equation (3.27) has the very same physical contents as the continuous-time differential equation (1.1). As an illustration of this point, the mean-squared position  $M_2^{(0)}(t)$  still obeys the ballistic law (2.14), albeit with a prefactor given by

$$a_2 = \int_B \frac{dp}{2\pi} \frac{4 \sin^2 p}{1 - 4\varepsilon^2 \cos^2 p} = \frac{1 - (1 - 4\varepsilon^2)^{1/2}}{\varepsilon^2} = 2 + 2\varepsilon^2 + \dots \quad (3.30)$$

The value  $a_2 = 2$ , characteristic of the continuous-time equation (see equations (2.14), (2.16)), is thus recovered, with a small correction in  $\varepsilon^2$ .

We have performed numerical simulations of the difference equation (3.27), with a timestep  $\varepsilon = 0.05$ , so that the oscillations and other discretization effects are negligible. The random site potentials have been drawn from a uniform distribution over the interval  $-W/2 < v_n < W/2$ , so that  $\sigma^2 = W^2/12$  and

$$\xi_0 \approx \frac{96}{W^2}. \quad (3.31)$$

The data to be presented below correspond to the following 10 values of the localization length scale:

$$\xi_0 = 25, 35, 50, 70, 100, 140, 200, 280, 400, 560. \quad (3.32)$$

For each value of  $\xi_0$ , the strength of disorder  $W$  is taken from the perturbative relation (3.31). The measured quantities are averaged over 1000 independent realizations of the random potentials. For each realization, equation (3.27) is integrated up to a time  $t_{\max} = 5\xi_0$ , in order to enter into the localized regime, and for a range of space  $|n| \leq n_{\max}$ , with  $n_{\max} = 2.5t_{\max} = 12.5\xi_0$ , in order to fully encompass the ballistic fronts.

*3.4.1. Moments of the position.* We have first checked the validity of the scaling law (3.18) for the moments  $M_q(t)$  of the position of the particle, as well as the analytical predictions concerning the associated scaling functions, on the examples of  $q = 2$  and  $q = 4$ . Figures 2 and 3 respectively show log-log plots of numerical data for  $M_2(t)$  and  $M_4(t)$ , divided by their expressions (2.14) in the absence of disorder, against the scaling variable  $x = t/\xi_0$ . The data, corresponding to the six largest values of equation (3.32) for  $\xi_0$ , collapse in a nice way. This demonstrates the existence of the one-variable scaling functions  $F_2(x)$  and  $F_4(x)$ .

The broken curves show the linear correction (3.20), (3.21) of the scaling functions at small  $x$ , as well as their asymptotic behaviour (3.19) at large  $x$ , namely  $F_2(x) \approx 0.4508/x^2$  and  $F_4(x) \approx 2.589/x^4$ . The full curves show the one-parameter phenomenological fits  $F_2(x) = (1 + 3.395x + 0.154x \ln(x + 1) + 2.218x^2)^{-1}$  and  $F_4(x) = (1 + 1.4336x + 0.622x \ln(x + 1) + 0.6215x^2)^{-2}$ . These expressions incorporate the small- $x$  and large- $x$  behaviour recalled just above. The fitted parameters are the amplitudes of the  $x \ln(x + 1)$  terms, reflecting the structure in  $(\ln x)/x$  of the leading correction term at large  $x$  discussed below equation (3.21). The good quality of the fits shows the quantitative agreement between analytical predictions and numerical data. We have also checked that the amplitudes of the behaviour (3.19), (3.20) of the scaling functions at small and large  $x$  are recovered within better than 10% if they are left as free fitting parameters, instead of being imposed as constraints.

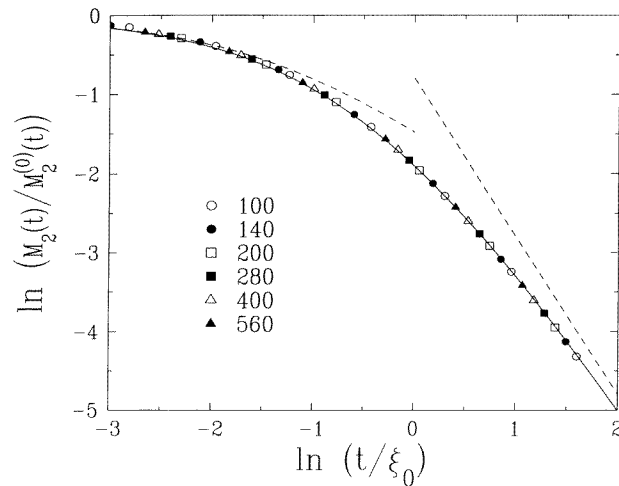


**Figure 2.** Log-log plot of the ratio of mean-squared position  $M_2(t)$  to its value  $M_2^{(0)}(t)$  in the absence of disorder, against the scaling variable  $x = t/\xi_0$ . Symbols: numerical data for various values of  $\xi_0$ . Phenomenological fit (full curve) and asymptotic behaviour (broken curves) are given in the text.

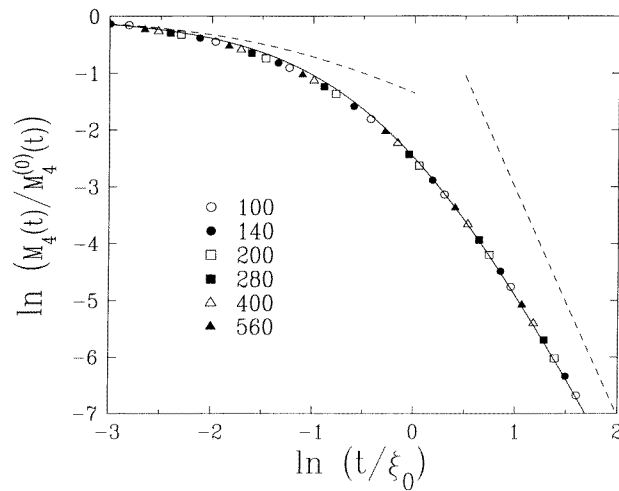


**Figure 3.** Same as figure 2, for the fourth moment  $M_4(t)$  of the position.

**3.4.2. Moments of the probability density (participation numbers).** We now turn to the moments  $S_q(t)$  of the probability density, for which fewer analytical predictions are available. We have first investigated the anomalous scaling laws of these moments in the localized regime, on the example of  $q = 3$ . In order to check the power law (3.15), as well as the leading correction to it, which can be expected to be of relative order  $\xi_0^{-1/3}$ , we have plotted in figure 4 the product  $\xi_0^2 S_3(\infty)$  against  $\xi_0^{1/3}$ . The data points correspond to all the values of equation (3.32) for  $\xi_0$ . For each  $\xi_0$ , the data for  $S_3(t)$  in the range  $1 \leq t/\xi_0 \leq 5$  have been extrapolated, in order to get a reliable estimate for  $S_3(\infty)$ . The error bars on the numbers obtained in this way are comparable to the symbol size. The plotted data nicely follow the least-square fit  $y = 2.46x - 2.21$ , confirming thus both the

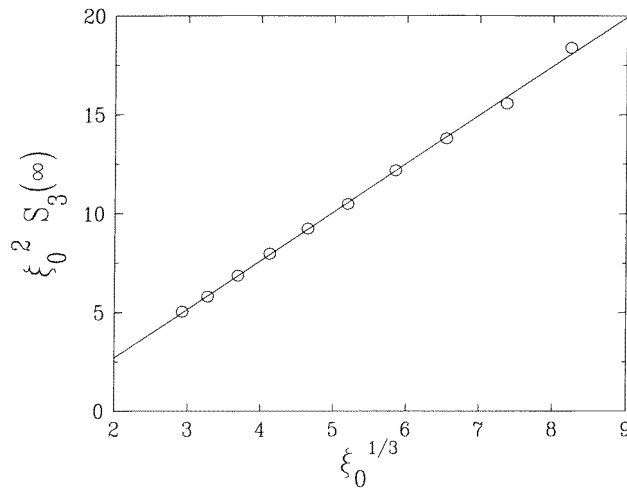


**Figure 4.** Plot of the product  $\xi_0^2 S_3(\infty)$  against  $\xi_0^{1/3}$ . Symbols: numerical data for various values of  $\xi_0$ . The least-square fit (full curve) is given in the text.

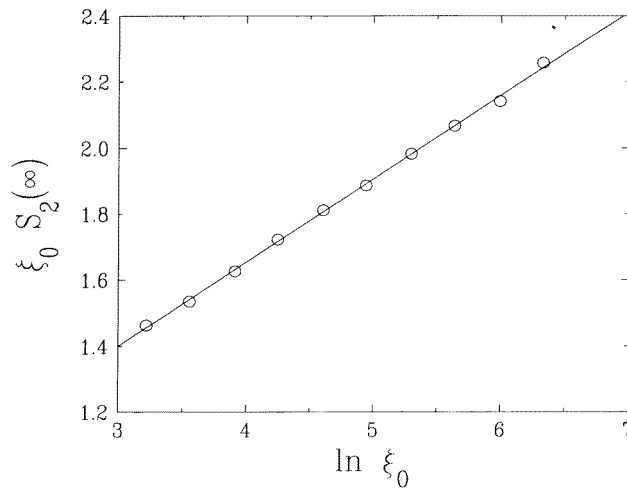


**Figure 5.** Same as figure 4, for the product  $\xi_0 S_2(\infty)$  against  $\ln \xi_0$ .

power-law behaviour (3.15) and the anticipated nature of the correction term, and yielding the estimate

$$B_3 \approx 2.5. \tag{3.33}$$

In order to check the logarithmic behaviour (3.16) of the participation number in the localized regime, we have plotted in figure 5 the product  $\xi_0 S_2(\infty)$  against  $\ln \xi_0$ . The data points have been obtained as those of figure 4. They nicely follow the least-square fit  $y = 0.253x + 0.642$ , confirming thus the behaviour (3.16), and yielding the estimates

$$\lambda \approx 0.25 \quad \mu \approx 0.64. \tag{3.34}$$

We have then determined the full one-variable scaling functions, defined in equation (3.22), for the participation numbers throughout the crossover from the ballistic



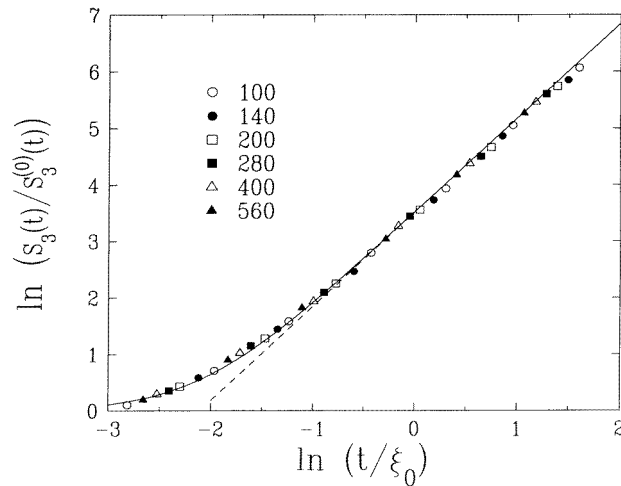


**Figure 6.** Log–log plot of the ratio of the participation number  $S_3(t)$  to its value  $S_3^{(0)}(t)$  in the absence of disorder, against the scaling variable  $x = t/\xi_0$ . Symbols and curves as in figure 2.

to the localized regime. We have again considered the example of  $q = 3$ . Figure 6 shows a log–log plot of  $S_3(t)$ , divided by its behaviour (2.19), (2.23) in the absence of disorder, against the scaling variable  $x = t/\xi_0$ . The data, corresponding to the six largest values of equation (3.32) for  $\xi_0$ , again collapse in a nice way, demonstrating the existence of the scaling function  $G_3(x)$ . The asymptotic large- $x$  behaviour  $G_3(x) \approx 33.6x^{5/3}$ , shown as a broken curve, is accurately obeyed for values of the scaling variable as small as  $x \approx 0.5$ . The full curve shows the one-parameter phenomenological fit  $G_3(x) = (1 - 0.56x + 67.8x^2)^{5/6}$ , with the fitted parameter being the amplitude of the middle term.

We end up with an investigation of the logarithmic behaviour (3.24) of the participation number  $S_2(t)$ , for generic values of the scaling variable  $x$ . To do so, for any fixed value of the ratio  $x = t/\xi_0$ , we have performed a least-square fit of all the available data for  $tS_2(t)$  against  $\ln t$ , the slope and the intercept of those fits respectively yielding estimates for  $\phi(x)$  and  $\chi(x)$ . Figure 7 shows a log–log plot of the amplitude  $\phi(x)$  thus obtained, against the scaling variable  $x$ . Broken curves show the value of  $\phi(0)$  given in equation (3.25), and the asymptotic behaviour  $\phi(x) \approx 0.253x$  (see equation (3.26)). The full curve shows the one-parameter phenomenological fit  $\phi(x) = (0.00257 + 0.00282x + 0.0639x^2)^{1/2}$ , with the fitted parameter being again the amplitude of the middle term. Similar, albeit less accurate, numerical results have been obtained for the function  $\chi(x)$ .

#### 4. Discussion

The most salient outcomes of this work are summarised in table 1. In the absence of disorder, and for an initially localized wavepacket, the probability density of a tight-binding particle exhibits anomalous scaling and bifractality. Indeed its moments of order  $q$ , namely the dynamical participation numbers  $S_q(t)$ , scale in time with a non-trivial exponent  $\tau(q)$  for  $q > 2$ .

To put it more boldly, a free quantum mechanical particle is bifractal. This striking feature is entirely due to the presence of ballistic fronts. For the tight-binding model considered in this paper, these fronts correspond to the transition region in the theory of

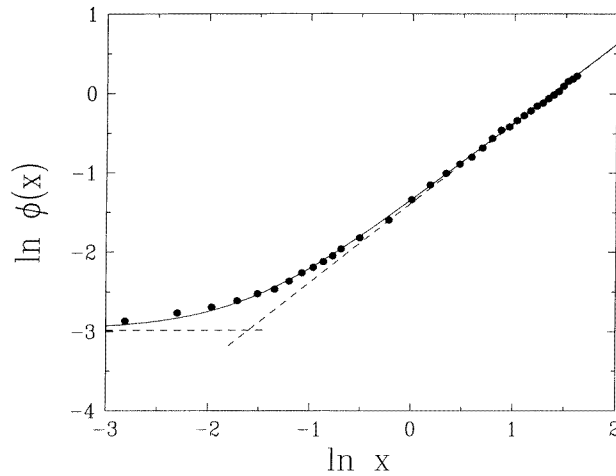


**Figure 7.** Log–log plot of the amplitude  $\phi(x)$  of the participation number  $S_2(t)$ , defined in equation (3.24), against the scaling variable  $x = t/\xi_0$ . Symbols: numerical data. Curves: as in figure 2.

Bessel functions. Both the existence of ballistic fronts and their width scaling as  $t^{1/3}$  are actually general characteristics of difference equations, with a bounded energy dispersion curve. To the best of our knowledge, this bifractality phenomenon has been overlooked so far. Plots similar to our figure 1, showing the squared Bessel function with its ballistic fronts, have been displayed and described e.g. in [25], but without the authors noticing the relevance of the fronts. The moments  $M_q(t)$  of the position of the particle are not affected at all by the presence of ballistic fronts. [5] contains a rigorous and general discussion on the spreading of a wavepacket.

For the Anderson model with a weak diagonal disorder, the bifractal phenomenon persists throughout the different regimes of the localization phenomenon. Indeed anomalous scaling of the participation numbers, with the same exponent  $\tau(q)$ , holds in the ballistic regime ( $t \ll \xi_0$ ), in the localized regime ( $t \gg \xi_0$ ), and in the crossover between them ( $t \sim \xi_0$ ), where these quantities obey scaling laws involving the single variable  $x = t/\xi_0$ . These scaling predictions have been confirmed quantitatively by accurate numerical simulations.

The bifractal exponent  $\tau(q)$  characterizes both the time decay of participation numbers in the ballistic case, and their dependence on  $\xi_0$  in the localized regime. In the ballistic regime ( $t \ll \xi_0$ ), this phenomenon is related to the existence of a finite upper band edge, and to the uniform scaling of single eigenstates. This absence of multifractality is in turn related to the direct crossover between a ballistic and a localized regime in the one-dimensional geometry, without an intermediate diffusive phase. These features have been established by means of a variety of analytical techniques [7, 8, 13–18]. In the localized regime ( $t \gg \xi_0$ ), bifractality is intimately related to the Derrida–Gardner anomalous scaling of the localization length and of the density of states near band edges.

Two very different physical mechanisms seem therefore to be responsible for the bifractal behaviour observed in these two different regimes. Let us underline that both phenomena have nevertheless one important characteristic in common. They take place near the band edges of the energy spectrum (2.2) in the absence of disorder, where the two plane waves  $\exp(\pm inp)$  become identical. This degeneracy of the plane-wave basis explains, at least

qualitatively, both the flatness of the dispersion curve around the upper band edge (hence the existence of sharp ballistic fronts) and the high sensitivity of eigenstates to a perturbation (hence the Derrida–Gardner anomalous scaling).

The usual participation number  $S_2(t)$  corresponds to the borderline case ( $q = 2$ ) between the normal and the anomalous regime. This quantity exhibits a logarithmic correction, either in time (see equation (2.29)) or in  $\xi_0$  (see equation (3.16)). A similar logarithmic behaviour has been described [26] in the case of the mean return probability

$$C(t) = \frac{1}{t} \int_0^t P_0(u) du. \quad (4.1)$$

In the absence of disorder, this quantity has a logarithmic correction to the naive scaling  $C^{(0)}(t) \sim 1/t$ , which can be easily derived by the Mellin approach, yielding

$$C^{(0)}(t) = \frac{1}{t} \int_0^t (J_0(2u))^2 du \approx \frac{\ln t + 4 \ln 2 + \gamma_E}{2\pi t} \quad (4.2)$$

a result very similar to equation (2.29). This behaviour was shown in [26] to explain the occurrence at several places in the literature of a fake non-trivial decay exponent  $\delta \approx 0.84$  for the mean return probability, even in the absence of disorder, as well as a variety of erroneous conclusions drawn from there.

Beyond the amusing phenomenon of bifractality demonstrated in the one-dimensional Anderson model, the present work underlines that the moments of the position of a quantum mechanical particle and the moments of the associated probability density (participation numbers) can exhibit different scaling laws, with unrelated dynamical exponents. This outcome corroborates the recent general discussion [5] on the complexity of the scaling laws governing the dynamics of quantum systems.

## Acknowledgments

It is a pleasure for us to thank J L Pichard and X Waintal for interesting discussions, and especially Y Fyodorov for an illuminating conversation.

## References

- [1] Lifshitz I M, Gredeskul S A and Pastur L A 1988 *Introduction to the Theory of Disordered Systems* (New York: Wiley)
- [2] Crisanti A, Paladin G and Vulpiani A 1992 *Products of Random Matrices in Statistical Physics* (Berlin: Springer)
- [3] Luck J M 1992 *Systèmes Désordonnés Unidimensionnels* (Collection Aléa-Saclay)
- [4] Sebbah P, Sornette D and Vanneste C 1993 *Phys. Rev. B* **48** 12506
- [5] Ketzmerick R, Kruse K, Kraut S and Geisel T 1997 *Phys. Rev. Lett.* **79** 1959
- [6] Huckestein B and Klesse R 1998 *Preprint cond-mat/9805038* and references therein
- [7] Mirlin A D and Fyodorov Y V 1993 *J. Phys. A: Math. Gen.* **26** L551  
Fyodorov Y V and Mirlin A D 1995 *Phys. Rev. B* **52** R11580
- [8] Frahm K and Müller-Groeling A 1995 *Europhys. Lett.* **32** 385
- [9] Izrailev F M, Kottos T, Politi A, Ruffo S and Tsironis G P 1996 *Europhys. Lett.* **34** 441  
Izrailev F M, Kottos T, Politi A and Tsironis G P 1997 *Phys. Rev. E* **55** 4951 and references therein
- [10] Borgonovi F and Shepelyansky D L 1996 *J. Physique I* **6** 287  
Evangelou S N, Xiong S J and Economou E N 1996 *Phys. Rev. B* **54** 8469  
Frahm K, Müller-Groeling A and Pichard J L 1996 *Phys. Rev. Lett.* **76** 1509  
Waintal X and Pichard J L 1997 *Preprint cond-mat/9706258* (*Eur. J. Phys. B* to appear)  
Waintal X, Weinmann D and Pichard J L 1998 *Preprint cond-mat/9801134* (*Eur. J. Phys. B* to appear)  
De Toro Arias S, Waintal X and Pichard J L 1998 *Preprint cond-mat/9808136*

- [11] Thouless D J 1974 *Phys. Rep.* **13** 93
- [12] Wegner F 1980 *Z. Phys. B* **36** 209
- [13] Kolokolov I V 1993 *Sov. Phys.-JETP* **76** 1099  
Kolokolov I V 1994 *Europhys. Lett.* **28** 193
- [14] Berezinskii V L 1974 *Sov. Phys.-JETP* **38** 620
- [15] Gogolin A A, Mel'nikov V I and Rashba E I 1976 *Sov. Phys.-JETP* **42** 168
- [16] Gogolin A A 1976 *Sov. Phys.-JETP* **44** 1003
- [17] Nakhmedov E P, Progodin V N and Firsov A Yu 1987 *Sov. Phys.-JETP* **65** 1202
- [18] Sheng P (ed) 1990 *Scattering and Localization of Classical Waves in Random Media* (Singapore: World Scientific)
- [19] Erdélyi A (ed) 1953 *Higher Transcendental Functions (The Bateman Manuscript Project)* (New York: McGraw-Hill)
- [20] Paladin G and Vulpiani A 1987 *Phys. Rep.* **156** 147  
Feder J 1988 *Fractals* (New York: Plenum)
- [21] Derrida B and Gardner E J 1984 *J. Physique I* **45** 1283
- [22] Schreiber M and Grussbach H 1991 *Phys. Rev. Lett.* **67** 607  
Evangelou S N and Katsanos D E 1993 *J. Phys. A: Math. Gen.* **26** L1243
- [23] Luck J M unpublished
- [24] Derrida B and Luck J M 1983 *Phys. Rev. B* **28** 7183
- [25] Katsanos D E, Evangelou S N and Xiong S J 1995 *Phys. Rev. B* **51** 895
- [26] Zhong J X and Mosseri R 1995 *J. Phys.: Condens. Matter* **7** 8383